

Ab initio study on some new spin-gapless
semiconductors: The Zr-based quaternary Heusler
alloys

Qiang Gao^a, Huan-Huan Xie^a, Lei Li^a, Gang Lei^a, Ke Wang^a, Jian-Bo
Deng^a, Xian-Ru Hu^{a,*}

^a*School of Physical Science and Technology, Lanzhou University, Lanzhou 730000,
People's Republic of China*

Abstract

Employing *ab initio* electronic structure calculations, we have investigated electronic and magnetic properties of the Zr-based quaternary Heusler alloys: ZrCoVIn, ZrFeVGe, ZrCoFeP, ZrCoCrBe and ZrFeCrZ (Z=In and Ga). Our *ab initio* calculation results show that all the alloys are (or nearly) spin-gapless semiconductors. All the alloys have large band gaps, indicating the stability of them at room temperature. The Slater-Pauling behaviours of these alloys are discussed as well. The values of Curie temperature of all the alloys are estimated. And it is found that the values of the Curie temperature for all our calculated quaternary Heusler alloys are higher than that of room temperature.

*Corresponding author

Email address: huxianru@lzu.edu.cn (Xian-Ru Hu)

Keywords: A. intermetallic compounds, semiconductors; B. magnetic properties; D. electronic structure;

1. Introduction

Efficient spin injection from a ferromagnet to a semiconductor is very meaningful for the development of the performance of spintronic devices [1]. Since the prediction of HM ferromagnetism of Heusler alloy NiMnSb by *ab initio* calculations in 1983 [2], half metallic ferromagnetism (HMF) has attracted great interest [3, 4, 5, 6]. And the half metallic ferromagnetic Heusler alloys are good candidates for the application of spintronic devices, as these alloys often have high spin polarization, high Curie temperature compatible lattice structure. The improvement of computer science makes it possible to design materials on computers, which is efficient and less cost [7, 8, 9]. Especially, computational material science enables the study of the new materials [8, 9], which is useful to the experiments and practical applications.

Recent studies have shown that there is a new class of materials, namely, spin-gapless semiconductors (SGS) [10, 11, 12]. SGS was first predicted in diluted magnetic semiconductors PbPdO₂ by *ab initio* calculations [10]. The excited carriers can be 100% spin polarized with tunable capabilities, and the SGS may be more practical in the use of spintronic applications than

half metals (HM). But there is a drawback that the Curie temperature (T_C) of this material is almost 180 K [13, 14]. As is known the Heusler alloys often have high T_C , the Heusler alloys may be a realization of SGS. And the Heusler compound Mn_2CoAl was first predicted to be a SGS with a high T_C of 720 K [11]. So the Heusler alloys are promising candidates for the future SGS use.

The Heusler alloys consist of Zr element have attracted great interest. There are many theoretical and experimental studies on the semi-Heusler alloy $ZrNiSn$ recently [15, 16, 17, 18]. Some investigations have shown that the Heusler alloys Co_2ZrSn [19, 20], Ni_2ZrSn [19], Ni_2ZrAl [21], Co_2ZrGe [22] and $ZrCoSb$ [23] are half metals. And many other interesting properties have been found, for example, the alloy $ZrPd_2Al$ is found to be superconductive [24].

In recent reports [25, 26, 27, 28, 29, 30], some so-called $LiMgPdSn$ or Y-type structure Heusler alloys with a formula of X_1X_2YZ have been discovered to be HMs by density function theory (DFT). Among the new structure Heusler alloys, $MnCrVAl$, $MnCrTiSi$, $CoFeCrAl$, $CoFeTiAs$, $CoMnCrSi$, $MnVTiAs$, $FeVTiAs$, $FeCrTiAl$, $CrVTiAl$, $CoVTiAl$, $CoFeMnSi$, $CoFeCrAl$ and $CoFeVSi$ are (or nearly) SGSs [31, 32]. As reported in **Refs.** [11, 33, 34, 35], the ternary Heusler alloys Ti_2MnZ ($Z=Al, Ga$ and In), Mn_2CoAl , Ti_2CoSi

and Ti_2VAs are (or nearly) also SGSs.

The Zr-Ti coupling quaternary Heusler alloys, ZrFeTiZ ($Z=\text{Al}$, Si and Ge) and ZrNiTiAl have been reported to be HMF very recently [36]. This is the first prediction of HMF in the 4d-3d transition metal elements coupling quaternary Heusler alloys. As reported, these alloys have large half metallic band gaps and spin flip gaps. But they are just normal HMFs not SGSs.

It is very interesting that the Zr-Ti coupling quaternary Heusler alloys have large HM band gaps and spin flip gaps, which means these alloys may be stable at room temperature. And there may be other Zr-based quaternary Heusler alloys with large HM band gaps, some probably being SGSs. Motivated by the above, we have designed the new Zr-based quaternary Heusler alloys: ZrCoVIn , ZrFeVGe , ZrCoFeP , ZrCoCrBe and ZrFeCrZ ($Z=\text{In}$ and Ga). The electronic and magnetic properties of the alloys are investigated by *ab initio* calculations. ZrCoVIn , ZrCoCrBe , ZrCoFeP and ZrFeCrIn also have large band gaps of 0.98 eV, 0.71 eV, 0.41 eV and 0.80 eV. ZrFeCrGa and ZrFeVGe are semiconductors. The calculation results show that ZrCoVIn , ZrCoCrBe , ZrFeVGe , ZrCoFeP , ZrFeCrIn and ZrFeCrGa are (or nearly) SGSs. The Slater-Pauling behaviours of these alloys are discussed in detail. The values of Curie temperature of all the alloys are estimated.

It is found that the values of the Curie temperature for all our calculated quaternary Heusler alloys are higher than that of room temperature. This means that all the calculated quaternary Heusler alloys keep being SGSs at room temperature and they may be practical in the future SGS use.

2. Methods and details

The lattice optimization, electronic density of states (DOS), magnetic moment and band structure of the new Zr-based quaternary Heusler alloys are calculated by employing *ab initio* method. All our *ab initio* calculations are performed by using the full-potential local-orbital minimum-basis band structure scheme (FPLO) [37, 38] with generalized gradient approximation (GGA)[39, 40, 41]. For the irreducible Brillouin zone, we use the k meshes of $20 \times 20 \times 20$ for all the calculations. The convergence criteria of self-consistent iterations is set to 10^{-6} to the density and 10^{-8} Hartree to the total energy per formula unit.

As described in Refs. [25, 26], the quaternary Heusler alloys has a so-called LiMgPdSn or Y-type structure (space group No.216, $F\bar{4}3m$). So all our calculations are performed in this lattice structure.

3. Results and Discussions

In general, the quaternary Heusler alloys have a formula of X_2YX_1Z . In our calculations, the X_2 atom is Zr atom and Z is a main group element atom. X_1 and Y are the 3d transition metal element atoms, which the atomic number X_1 is smaller than that of Y. According to group theory, the LiMgPdSn or Y-type structure quaternary Heusler alloys have four Wyckoff positions: 4a (0, 0, 0), 4b ($\frac{1}{2}, \frac{1}{2}, \frac{1}{2}$), 4c ($\frac{1}{4}, \frac{1}{4}, \frac{1}{4}$) and 4d ($\frac{3}{4}, \frac{3}{4}, \frac{3}{4}$). The lattice structure is face centered cubic (FCC). In principle, the X_1 , X_2 , Y and Z atoms can occupy one of the 4a, 4b, 4c and 4d positions. By interchanging the positions of atoms in LiMgPdSn or Y-type structure quaternary Heusler alloys, three possible types of atom arrangement are formed: Y-type (*I*), Y-type (*II*) and Y-type (*III*). Zr, Y, X_1 and Z atoms are arranged at different positions Y-type (*I*)=(4a, 4b, 4c, 4d), Y-type (*II*)=(4a, 4b, 4c, 4d) and Y-type (*III*)=(4a, 4b, 4d, 4c). In order to get the equilibrium structures of the Zr-based quaternary Heusler alloys, the geometry optimization are firstly performed in their three different configurations by calculating the total energies as a function of lattice constants. From the calculated results of total energies at equilibrium lattice constants, we find that Y-type (*I*) is the most stable one of the three structures for both spin-polarization (FM

phase) and non-spin-polarization (NM phase). And FM phase is more stable than NM phase in Y-type (*I*). This is in agreement with the previous papers [25, 26, 27, 28, 36]. The obtained equilibrium of lattice results in Y-type (*I*) are presented in **Table 1** for the FM phases. So we will only discuss the quaternary Heusler alloys in Y-type (*I*) structure for the FM phases.

3.1. Slater-Pauling behaviours

Table 2 shows the magnetic moment of all our calculated alloys under the equilibrium lattice constants.

All the calculated quaternary Heusler alloys have very large band gaps. It means they may keep their magnetic properties at room temperature.

We will have a brief discussion of the Slater-Pauling behaviours based on the values of total magnetic moment in **Table 2**. The calculated total magnetic moment per formula unit, $3 \mu_B$, for the quaternary Heusler alloys ZrCoVIn, ZrCoCrBe, ZrFeCrIn, ZrFeCrGa and ZrFeVGe, obeys the Slater-Pauling behaviour which can be expressed by,

$$M_{tot} = (Z_{tot} - 18)\mu_B \quad (1)$$

here M_{tot} and Z_{tot} are the total magnetic moment per formula unit and

the number of total valence electrons in each the above alloys. Z_{tot} is 21. The values of magnetic moment per formula unit is $2 \mu_B$ for the calculated quaternary Heusler alloys ZrCoFeP. The Slater-Pauling behaviour which is obeyed by ZrCoFeP can be expressed by,

$$M_{tot} = (Z_{tot} - 24)\mu_B \quad (2)$$

here M_{tot} and Z_{tot} have the same meaning as previous. The value of Z_{tot} is 26.

The investigations of the Slater-Pauling behaviours of usual full and inverse Heusler alloys can be found in Refs. [42, 43]. Similar to the discussions in Refs. [42, 43], we present the possible hybridizations between minority - spin d orbitals at different occupations in the case of 21 and 26 valence electrons in **Figure 1** and **Figure 2**. As described in **Ref [42]** for both figures, $d_{1,\dots,5}$ orbitals correspond to the d_{xy} , d_{yz} , d_{zx} , $d_{3z^2-r^2}$ and $d_{x^2-y^2}$ orbitals, respectively.

Figure 1 is in corresponding to the alloys ZrCoVIn, ZrCoCrBe, ZrFeCrIn, ZrFeCrGa and ZrFeVGe. For these alloys, the 3d transition metallic elements X₁ and Y sit at the sites with the same symmetry, so their 3d or-

bitals hybridize similar to which described in **Refs.** [42, 43]. The 3d orbitals of X_1 and Y atoms hybridize, creating five 3d bonding and nonbonding states. And the five X_1 -Y bonding states hybridize with the 4d orbitals of the Zr atom, creating again bonding and antibonding states. Similar to the Sc_2 and Ti_2 based inverse Heusler compounds[43], the triple-degeneration t_{1u} states and the double-degeneration e_u states are in very high energy level. So both the t_{1u} and e_u states are empty. And the spin-down gap is created between the non-bonding t_{1u} states and the bonding t_{2g} state. As can be seen in **Figure 1**, one bonding t_{2g} state and e_g state are below the Fermi level in the hybridization schematic. The un-shown $1 \times s$ state and $3 \times p$ state are also below the Fermi level. In total there are 9 states below Fermi level. The total magnetic moment M_{tot} (in μ_B) is just the difference between the number of occupied spin-up states and occupied spin-down states. We can directly deduce the number of occupied spin-up states: $N \uparrow = Z_{tot} - N \downarrow$. So the total magnetic moment: $M_{tot} = (N \uparrow - N \downarrow)\mu_B = (Z_{tot} - 2 \times N \downarrow)\mu_B = (Z_{tot} - 18)\mu_B$. So the Heusler alloys ZrCoVIn, ZrCoCrBe, ZrFeCrIn, ZrFeCrGa and ZrFeVGe obey the Slater-Pauling behaviour expressed by **Equation(1)**.

As for ZrCoFeP, we should focus on the hybridization schematic in **Figure 2**. X_1 , Y and Z are Fe, Co and P, respectively. This case is similar to the full-

Heusler alloys.[42] As can be seen in **Figure 2**, the t_{1u} state is below Fermi level and e_u state is above Fermi level. The the spin-down gap is created between the nonbonding t_{1u} and e_u states. From **Figure 2**, we can get that t_{2g} and e_g states are below Fermi level. Considering the $1 \times s$ and $3 \times p$ states, there are 12 states below Fermi level in total. We can directly deduce the total magnetic moment: $M_{tot} = (N \uparrow - N \downarrow)\mu_B = (Z_{tot} - 2 \times N \downarrow)\mu_B = (Z_{tot} - 24)\mu_B$. That is why ZrCoFeP obeys the Slater-Pauling behaviour expressed by **Equation(2)**.

It is very interesting that the number of the valence electrons for our calculated spin-gapless semiconductors (SGS) is either 21 or 26, which is similar to the results described in **Ref [31]**. And the Slater-Pauling behaviours obeyed by our calculated SGSs are also similar to the discussions in **Ref [31]**.

3.2. Electronic structure properties

In this section, we will discuss the properties of spin-gapless semiconductors (SGS). **Figure 3** shows the total density of states of all the calculated alloys. And **Figure 4** shows the partial density of states (PDOS) of ZrCoVIn under the equilibrium lattice constants of all our calculated quaternary Heusler alloys.

Firstly, we focus on the total DOS. In each of the cases, there is a large gap in the spin down band structure and the Fermi level falls within this gap. In the spin up band structure, for ZrCoVIn and ZrFeCrIn, the valence and conduction bands touch each other and the Fermi level falls within a zero-energy gap, which forms a valley in the spin up band structure. As described in **Refs.** [10], ZrCoVIn and ZrFeCrIn can be classified as SGSs. So no energy is required to excite electrons from the valence band to the conduction band, which is the same phenomenon that can be seen for the Hg-based gapless semiconductors and graphene [10]. And more interesting is that for an excitation energy up to the band gap energy of the spin channel and the holes can also be 100% spin polarized. So the carriers two can be possible fully polarized in the two SGSs. Therefore they can be used as spintronic materials with superior performance to half metals and diluted magnetic semiconductors [10, 11]. In the cases of ZrCoCrBe and ZrCoFeP, in the spin up band structure, there is a small overlap of the band being located and above and below the Fermi level although no band-crossing occurs. So the quaternary Heusler alloys ZrCoCrBe and ZrCoFeP are almost SGSs. In the case of ZrFeCrGa, it is clear to see there is a large band gap in the spin-down channel. And a close look at the band structure reveals that

there is a very narrow band gap of 0.02 eV. In the spin up band structure, the valence and conduction bands touch each other but the Fermi level falls within a narrow band gap. So ZrFeCrGa is very close to a SGS. In the case of ZrFeVGe, there is a large band gap in both spin down and up channels but the two gaps are not located at the same energy region. And a close look at the band structure reveals that there is a band gap below the Fermi level in the spin up band which touches the Fermi level resulting in an almost vanishing DOS below the Fermi level. So the Fermi level slightly crosses the spin-down conduction band and the spin-up valence band. As a result, the quaternary Heusler alloy ZrFeVGe can be classified as an indirect spin-gapless semiconductor.

Next the partial density of states (PDOS) will be discussed. From **Figure 4**, we can get that for the quaternary Heusler alloy ZrCoVIn, the 3d states of V and Co atoms make the most contributions to the total DOS near the Fermi levels. The 4d states of Zr make the most contributions to the total DOS of the Zr states near the Fermi levels. And the 5p states of In states make the most contributions to the total DOS near the Fermi levels of the Zr states. From the PDOS, it can be seen there are hybridizations between V-3d, Zr-4d and Co-3d states around the Fermi levels. We can get similar

conclusions for the other calculated alloys.

3.3. Curie temperature

As is known, the Curie temperature, T_C , of the magnetic materials is crucial for the practical applications. So in this section, we would comment on the expected Curie temperature.

The previous investigations on multi-sublattice half-metallic Heusler compounds have shown that Curie temperature is more or less proportional to total spin magnetic moment (or the sum of the absolute values of the atomic spin magnetic moments in the case of ferrimagnets) since Curie temperature is mainly determined by the nearest neighbor inter-sublattice exchange interactions [44, 45, 46, 47, 48, 49]. As described **in Refs.** [11, 33], it is found experimentally that the T_C of Mn_2CoAl is 720 K and the the sum of the absolute values of the spin moments is $5.47 \mu_B$. Based on the empirical value and according to **Table 2**, we can estimate that the value of T_C for the quaternary Heusler alloy ZrCoFeP is 320 K. As the sum of the absolute values of the atomic spin magnetic moments for ZrCoFeP is the lowest of all our calculated quaternary Heusler alloys, the values of T_C for all our calculated quaternary Heusler alloys are higher than that of room temperature. So the SGSs may probably be stable at room temperature. And they may

be candidates for the future spin-gapless semiconductors applications.

4. Conclusions

In conclusion, we have investigated some Zr-based quaternary Heusler alloys by employing *ab initio* calculations. It is found that the Zr-based quaternary Heusler alloys ZrCoVIn, ZrCoCrBe, ZrFeVGe, ZrCoFeP, ZrFeCrIn and ZrFeCrGa are (or nearly) SGSs with large band gaps by studying the DOS. The Slater-Pauling behaviours of these alloys are discussed as well. The Curie temperature for these alloys have also been estimated, and the results show that the values of the Curie temperature for these alloys are higher than that of room temperature. So these alloys can be the potential candidates for the future SGS applications.

References

- [1] I. Zutti, J. Fabian, S. Das Sarma, Spintronics: Fundamentals and applications, *Reviews of Modern Physics* 76 (2) (2004) 323–410. doi:10.1103/RevModPhys.76.323.
URL <http://link.aps.org/doi/10.1103/RevModPhys.76.323>
- [2] R. A. de Groot, F. M. Mueller, P. G. v. Engen, K. H. J. Buschow, New class of materials: Half-metallic ferromagnets, *Physical Review Letters* 50 (25) (1983) 2024–2027. doi:10.1103/PhysRevLett.50.2024.
URL <http://link.aps.org/doi/10.1103/PhysRevLett.50.2024>
- [3] J. Nehra, N. Lakshmi, K. Venugopalan, Effect of substitution of co with fe on the structural, electronic and magnetic properties of heusler compounds, *Physica B: Condensed Matter* 459 (2015) 46–51.
doi:10.1016/j.physb.2014.11.096.
URL <http://www.sciencedirect.com/science/article/pii/S0921452614009302>
- [4] N. Kervan, S. Kervan, Half-metallic properties in the fe₂tip full-heusler compound, *Intermetallics* 37 (2013) 88–91. doi:10.1016/j.intermet.2013.02.005.
URL <http://www.sciencedirect.com/science/article/pii/S096697951300040X>
- [5] T. Y. Wenxu Zhang, Band structure effects in rh₂tmsn full heusler

- compounds, *Journal of Alloys and Compounds* 618 (2015) 78–83.
doi:10.1016/j.jallcom.2014.08.146.
- [6] N. Mattern, W. X. Zhang, S. Roth, H. Reuther, C. Baehtz, M. Richter, Structural and magnetic properties of non-stoichiometric fe2zr, *Journal of Physics: Condensed Matter* 19 (37) (2007) 376202.
doi:10.1088/0953-8984/19/37/376202.
URL <http://iopscience.iop.org/0953-8984/19/37/376202>
- [7] T. A. Rokob, M. Srnec, L. Rulek, Theoretical calculations of physico-chemical and spectroscopic properties of bioinorganic systems: current limits and perspectives, *Dalton Transactions* (Cambridge, England: 2003) 41 (19) (2012) 5754–5768. doi:10.1039/c2dt12423h.
- [8] C. M. Handley, J. Behler, Next generation interatomic potentials for condensed systems, *The European Physical Journal B* 87 (7).
doi:10.1140/epjb/e2014-50070-0.
URL <http://epjb.epj.org/articles/epjb/abs/2014/07/b140070/b140070.html>
- [9] L. Lehtovaara, T. Kiljunen, J. Eloranta, Efficient numerical method for simulating static and dynamic properties of superfluid helium *Journal of Computational Physics* 194 (1) (2004) 78–91.

doi:10.1016/j.jcp.2003.08.020.

URL <http://www.sciencedirect.com/science/article/pii/S0021999103004613>

- [10] X. L. Wang, Proposal for a new class of materials: Spin gapless semiconductors,

Physical Review Letters 100 (15) (2008) 156404.

doi:10.1103/PhysRevLett.100.156404.

URL <http://link.aps.org/doi/10.1103/PhysRevLett.100.156404>

- [11] S. Ouardi, G. H. Fecher, C. Felser, J. Kbler,

Realization of spin gapless semiconductors: The heusler compound $\{\mathrm{Mn}\}_2\mathrm{m}$

Physical Review Letters 110 (10) (2013) 100401.

doi:10.1103/PhysRevLett.110.100401.

URL <http://link.aps.org/doi/10.1103/PhysRevLett.110.100401>

- [12] X. Hu, W. Zhang, L. Sun, A. V. Krasheninnikov,

Gold-embedded zigzag graphene nanoribbons as spin gapless semiconductors,

Physical Review B 86 (19) (2012) 195418.

doi:10.1103/PhysRevB.86.195418.

URL <http://link.aps.org/doi/10.1103/PhysRevB.86.195418>

- [13] H. Ohno, Making nonmagnetic semiconductors ferromagnetic, Science

281 (5379) (1998) 951–956. doi:10.1126/science.281.5379.951.

URL <http://www.sciencemag.org/content/281/5379/951>

- [14] M. Wang, R. P. Campion, A. W. Rushforth, K. W. Edmonds, C. T. Foxon, B. L. Gallagher, Achieving high curie temperature in (ga,mn)as, Applied Physics Letters 93 (13) (2008) 132103. doi:10.1063/1.2992200. URL <http://scitation.aip.org/content/aip/journal/apl/93/13/10.1063/1.2992200>
- [15] S. Populoh, M. H. Aguirre, O. C. Brunko, K. Galazka, Y. Lu, A. Weidenkaff, High figure of merit in (ti,zr,hf)NiSn half-heusler alloys, Scripta Materialia 66 (12) (2012) 1073–1076, WOS:000304641500026. doi:10.1016/j.scriptamat.2012.03.002.
- [16] R. A. Downie, D. A. MacLaren, J.-W. G. Bos, Thermoelectric performance of multiphase XNiSn (x = ti, zr, hf) half-heusler alloys, Journal of Materials Chemistry A 2 (17) (2014) 6107–6114, WOS:000333580700019. doi:10.1039/c3ta13955g.
- [17] H.-H. Xie, C. Yu, T.-J. Zhu, C.-G. Fu, G. J. Snyder, X.-B. Zhao, Increased electrical conductivity in fine-grained (zr,hf)NiSn based thermoelectric materials with nanoscale precipitates, Applied

- Physics Letters 100 (25) (2012) 254104, WOS:000305676400112.
doi:10.1063/1.4730436.
- [18] C. S. Birkel, J. E. Douglas, B. R. Lettiere, G. Seward, N. Verma, Y. Zhang, T. M. Pollock, R. Seshadri, G. D. Stucky, Improving the thermoelectric properties of half-Heusler TiNiSn through inclusion of a second full-Heusler phase: microwave preparation and spark plasma sintering of $\text{TiNi}_{1+x}\text{Sn}$, Physical Chemistry Chemical Physics 15 (18) (2013) 6990–6997, WOS:000317866300050. doi:10.1039/c3cp50918d.
- [19] S. Rauf, S. Arif, M. Haneef, B. Amin, The first principle study of magnetic properties of $\text{Mn}_2\text{W}_2\text{Sn}$, $\text{Fe}_2\text{Y}_2\text{Sn}$ ($y=\text{Ti}, \text{V}$), $\text{Co}_2\text{Y}_2\text{Sn}$ ($y=\text{Ti}, \text{Zr}, \text{Hf}, \text{V}, \text{Mn}$) and $\text{Ni}_2\text{Y}_2\text{Sn}$ ($y=\text{Ti}, \text{Zr}, \text{Hf}, \text{V}, \text{Mn}$) Heusler alloys, Journal of Physics and Chemistry of Solids 76 (2015) 153–169, WOS:000345183700021. doi:10.1016/j.jpcs.2014.07.021.
- [20] A. lebarski, A. Jeziarski, M. Neumann, S. Plogmann, Influence of vacancies on the electronic structure of Co ZrSn Heusler alloys, The European Physical Journal B - Condensed Matter and Complex Systems 12 (4) (1999) 519–523. doi:10.1007/s100510051034.
URL <http://link.springer.com/article/10.1007/s100510051034>

- [21] P. V. S. Reddy, V. Kanchana, Ab initio study of fermi surface and dynamical properties of Ni_2XAl ($x = \text{Ti, V, Zr, Nb, Hf}$ and Ta), *Journal of Alloys and Compounds* 616 (2014) 527–534, WOS:000342654000079. doi:10.1016/j.jallcom.2014.07.020.
- [22] S. Li, Y. Liu, Z. Ren, X. Zhang, G. Liu, Electronic structure and half-metallicity of the heusler alloy Co_2ZrGe , *Journal of the Korean Physical Society* 65 (7) (2014) 1059–1062, WOS:000344333300017. doi:10.3938/jkps.65.1059.
- [23] V. V. Romaka, L. Romaka, P. Rogl, Y. Stadnyk, N. Melnychenko, R. Korzh, Z. Duriagina, A. Horyn, Peculiarities of thermoelectric half-heusler phase formation in Zr-Co-Sb ternary system, *Journal of Alloys and Compounds* 585 (2014) 448–454, WOS:000327492600066. doi:10.1016/j.jallcom.2013.09.097.
- [24] T. Klimczuk, C. H. Wang, K. Gofryk, F. Ronning, J. Winterlik, G. H. Fecher, J.-C. Griveau, E. Colineau, C. Felser, J. D. Thompson, D. J. Safarik, R. J. Cava, Superconductivity in the heusler family of intermetallics, *Physical Review B* 85 (17) (2012) 174505, WOS:000303794300003. doi:10.1103/PhysRevB.85.174505.

- [25] P. Klaer, B. Balke, V. Alijani, J. Winterlik, G. H. Fecher, C. Felser, H. J. Elmers, Element-specific magnetic moments and spin-resolved density of states in CoFeMnZ ($Z=\text{Ti, V, Cr, Ni}$) Physical Review B 84 (14) (2011) 144413.
doi:10.1103/PhysRevB.84.144413.
URL <http://link.aps.org/doi/10.1103/PhysRevB.84.144413>
- [26] V. Alijani, S. Ouardi, G. H. Fecher, J. Winterlik, S. S. Naghavi, X. Kozina, G. Stryganyuk, C. Felser, E. Ikenaga, Y. Yamashita, S. Ueda, K. Kobayashi, Electronic, structural, and magnetic properties of the half-metallic ferromagnetic quaternary CoFeMnZ ($Z=\text{Ti, V, Cr, Ni}$) Physical Review B 84 (22) (2011) 224416.
doi:10.1103/PhysRevB.84.224416.
URL <http://link.aps.org/doi/10.1103/PhysRevB.84.224416>
- [27] L. Xiong, L. Yi, G. Y. Gao, Search for half-metallic magnets with large half-metallic gaps in CoFeMnZ ($Z=\text{Ti, V, Cr, Ni}$) Journal of Magnetism and Magnetic Materials 360 (2014) 98–103.
doi:10.1016/j.jmmm.2014.02.050.
URL <http://www.sciencedirect.com/science/article/pii/S0304885314001620>
- [28] G. Y. Gao, L. Hu, K. L. Yao, B. Luo, N. Liu,

- Large half-metallic gaps in the quaternary heusler alloys CoFeCrZ (z=al, si, ga, ge): A first-principles calculation
Journal of Alloys and Compounds 551 (2013) 539–543.
doi:10.1016/j.jallcom.2012.11.077.
URL <http://www.sciencedirect.com/science/article/pii/S0925838812020610>
- [29] G. Gkolu, Ab initio electronic structure of NiCoCrGa half-metallic quaternary heusler compounds
Solid State Sciences 14 (9) (2012) 1273–1276.
doi:10.1016/j.solidstatesciences.2012.07.013.
URL <http://www.sciencedirect.com/science/article/pii/S1293255812002348>
- [30] M. Singh, H. S. Saini, J. Thakur, A. H. Reshak, M. K. Kashyap,
Electronic structure, magnetism and robust half-metallicity of new quaternary heusler alloy HfCoFeCrGa
Journal of Alloys and Compounds 580 (2013) 201–204.
doi:10.1016/j.jallcom.2013.05.111.
URL <http://www.sciencedirect.com/science/article/pii/S0925838813012711>
- [31] K. Zdoan, E. Aolu, I. Galanakis, Slater-pauling behavior in LiMgPdSn-type multifunctional quaternary heusler compounds
Journal of Applied Physics 113 (19) (2013) 193903.
doi:10.1063/1.4805063.
URL <http://scitation.aip.org/content/aip/journal/jap/113/19/10.1063/1.4805063>
- [32] G. Z. Xu, E. K. Liu, Y. Du, G. J. Li, G. D. Liu, W. H. Wang, G. H. Wu,

A new spin gapless semiconductors family: Quaternary heusler compounds,
EPL (Europhysics Letters) 102 (1) (2013) 17007.
doi:10.1209/0295-5075/102/17007.
URL <http://iopscience.iop.org/0295-5075/102/1/17007>

[33] S. Skaftouros, K. zdoan, E. aolu, I. Galanakis,
Search for spin gapless semiconductors: The case of inverse heusler compounds,
Applied Physics Letters 102 (2) (2013) 022402.
doi:10.1063/1.4775599.
URL <http://scitation.aip.org/content/aip/journal/apl/102/2/10.1063/1.4775599>

[34] H. Y. Jia, X. F. Dai, L. Y. Wang, R. Liu,
X. T. Wang, P. P. Li, Y. T. Cui, G. D. Liu,
Ti₂mnz (z=al, ga, in) compounds: Nearly spin gapless semiconductors,
AIP Advances 4 (4) (2014) 047113. doi:10.1063/1.4871403.
URL <http://scitation.aip.org/content/aip/journal/adva/4/4/10.1063/1.4871403>

[35] K.-L. Y. G. Y. Gao, Antiferromagnetic half-metals, gapless half-
metals, and spin gapless semiconductors: The d03-type heusler
alloys, Applied Physics Letters 103 (23) (2013) 232409–232409–5.
doi:10.1063/1.4840318.

- [36] S. Berri, M. Ibrir, D. Maouche, M. Attallah,
First principles study of structural, electronic and magnetic properties of ZrFeTiAl, ZrFeTiSi
Journal of Magnetism and Magnetic Materials 371 (2014) 106–111.
doi:10.1016/j.jmmm.2014.07.033.
URL <http://www.sciencedirect.com/science/article/pii/S0304885314006441>
- [37] K. Koepnik, H. Eschrig, Full-potential nonorthogonal local-orbital minimum-basis band-structure
Physical Review B 59 (3) (1999) 1743–1757.
doi:10.1103/PhysRevB.59.1743.
URL <http://link.aps.org/doi/10.1103/PhysRevB.59.1743>
- [38] I. Opahle, K. Koepnik, H. Eschrig,
Full-potential band-structure calculation of iron pyrite, Physical Review B 60 (20) (1999) 14035–14041. doi:10.1103/PhysRevB.60.14035.
URL <http://link.aps.org/doi/10.1103/PhysRevB.60.14035>
- [39] D. C. Langreth, J. P. Perdew, Theory of nonuniform electronic systems. i. analysis of the gradient
Physical Review B 21 (12) (1980) 5469–5493.
doi:10.1103/PhysRevB.21.5469.
URL <http://link.aps.org/doi/10.1103/PhysRevB.21.5469>
- [40] J. P. Perdew, Density-functional approximation for the correlation energy of the inhomogeneous

Physical Review B 33 (12) (1986) 8822–8824.

doi:10.1103/PhysRevB.33.8822.

URL <http://link.aps.org/doi/10.1103/PhysRevB.33.8822>

- [41] J. P. Perdew, W. Yue, Accurate and simple density functional for the electronic exchange energy

Physical Review B 33 (12) (1986) 8800–8802.

doi:10.1103/PhysRevB.33.8800.

URL <http://link.aps.org/doi/10.1103/PhysRevB.33.8800>

- [42] I. Galanakis, P. H. Dederichs, N. Papanikolaou,

Slater-pauling behavior and origin of the half-metallicity of the full-Heusler alloys,

Physical Review B 66 (17) (2002) 174429.

doi:10.1103/PhysRevB.66.174429.

URL <http://link.aps.org/doi/10.1103/PhysRevB.66.174429>

- [43] S. Skafrouros, K. Zdoan, E. Aolu, I. Galanakis,

Generalized Slater-Pauling rule for the inverse Heusler compounds,

Physical Review B 87 (2) (2013) 024420.

doi:10.1103/PhysRevB.87.024420.

URL <http://link.aps.org/doi/10.1103/PhysRevB.87.024420>

- [44] E. Aolu, Nonzero macroscopic magnetization in half-metallic antiferromagnets at finite temperature

Physical Review B 79 (10) (2009) 100406.

doi:10.1103/PhysRevB.79.100406.

URL <http://link.aps.org/doi/10.1103/PhysRevB.79.100406>

[45] J. Ruz, L. Bergqvist, J. Kudrnovsk, I. Turek,

Exchange interactions and curie temperatures in $\{\mathrm{Ni}\}_{2-x}\mathrm{Mn}\}$

Physical Review B 73 (21) (2006) 214412.

doi:10.1103/PhysRevB.73.214412.

URL <http://link.aps.org/doi/10.1103/PhysRevB.73.214412>

[46] E. . I. Galanakis, High TC half-metallic fully-compensated ferrimag-

netic heusler compounds, Applied Physics Letters 99 (5) (2011) 052509–

052509–3. doi:10.1063/1.3619844.

[47] L. M. S. E. Sasioglu, First-principles study of exchange interactions

and curie temperatures of half-metallic ferrimagnetic full heusler alloys

mn₂vz (z=al, ge)doi:10.1088/0953-8984/17/6/017.

[48] J. Kbler, G. H. Fecher, C. Felser,

Understanding the trend in the curie temperatures of $\{\mathrm{Co}\}_{2}$ -based heusler c

Physical Review B 76 (2) (2007) 024414.

doi:10.1103/PhysRevB.76.024414.

URL <http://link.aps.org/doi/10.1103/PhysRevB.76.024414>

[49] E. aolu, L. M. Sandratskii, P. Bruno, I. Galanakis,

Exchange interactions and temperature dependence of magnetization in half-metallic heusler

Physical Review B 72 (18) (2005) 184415.

doi:10.1103/PhysRevB.72.184415.

URL <http://link.aps.org/doi/10.1103/PhysRevB.72.184415>

Table 1: The results of the lattice optimization of all our calculated quaternary Heusler alloys in $Y(I)$ structure for FM phase.

ZrYX ₁ Z	a_{opt} (Å)	E_{tot} (Ry)	band gap (eV)
ZrCoVIn	6.468	-23650.670779	0.98
ZrCoCrBe	6.013	-12116.709912	0.71
ZrFeCrIn	6.419	-23612.431029	0.80
ZrFeCrGa	6.184	-15734.120866	↑0.02 ↓0.71
ZrFeVGe	6.210	-15840.940640	↑0.41 ↓0.81
ZrCoFeP	5.944	-13215.295374	0.41

Table 2: The partial and total magnetic moments of all our calculated Heusler alloys in type (*I*) structure under the equilibrium lattice constant. M_{abs} is the sum of magnetic moments of all the atoms for each alloy.

ZrYX ₁ Z	$M_{X_1} (\mu_B)$	$M_{Zr} (\mu_B)$	$M_Y (\mu_B)$	$M_Z (\mu_B)$	$M_{tot} (\mu_B)$	$M_{abs} (\mu_B)$
ZrCoVIn	2.89	0.19	0.04	-0.12	3.00	3.25
ZrCoCrBe	3.21	-0.17	0.14	-0.18	3.00	3.72
ZrFeCrIn	3.45	-0.27	-0.03	-0.15	3.00	3.91
ZrFeCrGa	3.12	-0.29	0.32	-0.15	3.00	3.88
ZrFeVGe	2.58	0.00	0.57	-0.15	3.00	3.32
ZrCoFeP	1.19	-0.24	0.99	0.06	2.00	2.49

Figure captions

Figure 1: Possible hybridizations between spin-down orbitals siting at different sites in the case of 21 valence electrons for our calculated quaternary Heusler alloys.

Figure 2: Possible hybridizations between spin-down orbitals siting at different sites in the case of ZrCoFeP.

Figure 3: The total density of states (DOS) for all our calculated quaternary Heusler alloys.

Figure 4: The partial density of states (PDOS) for ZrCoVIn.

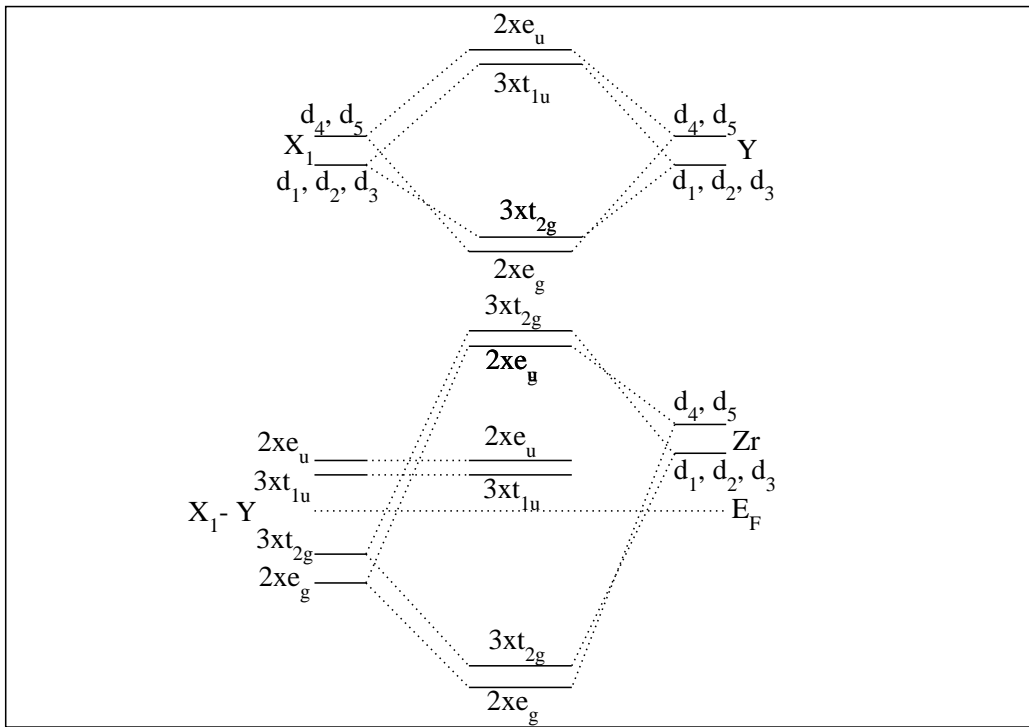


Figure 1:

Figures

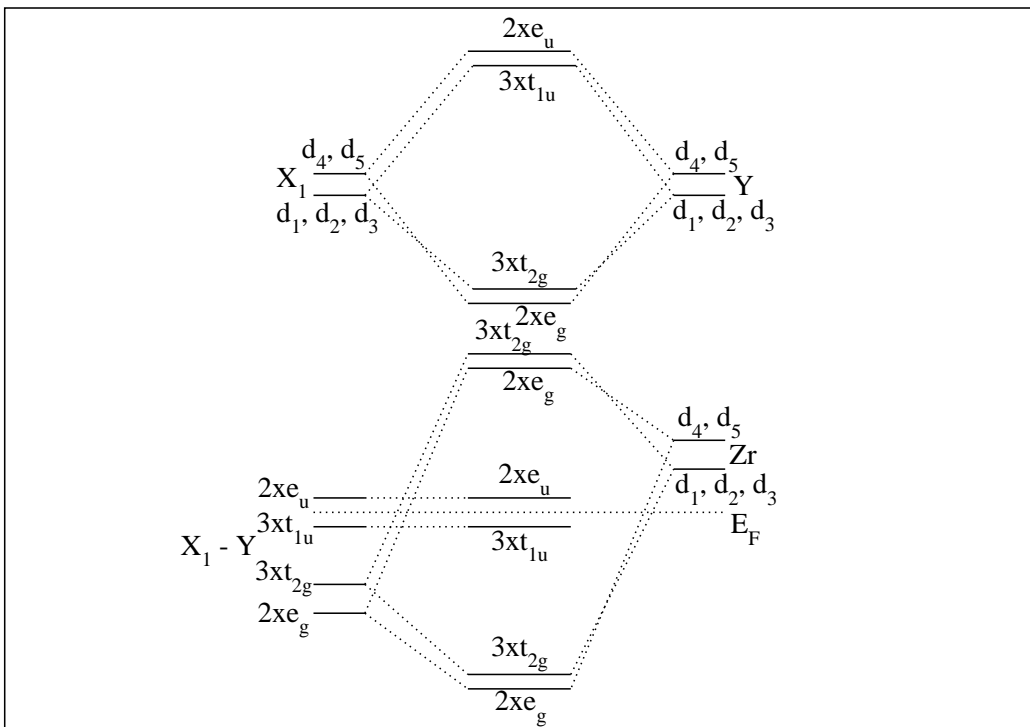


Figure 2:

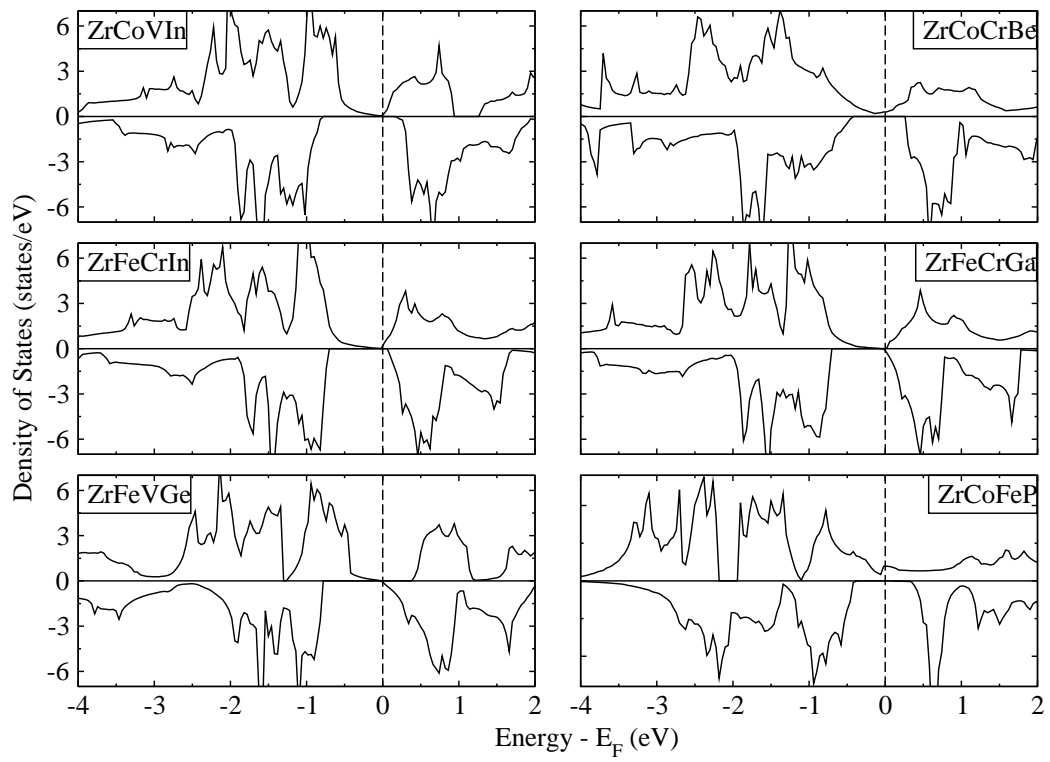


Figure 3:

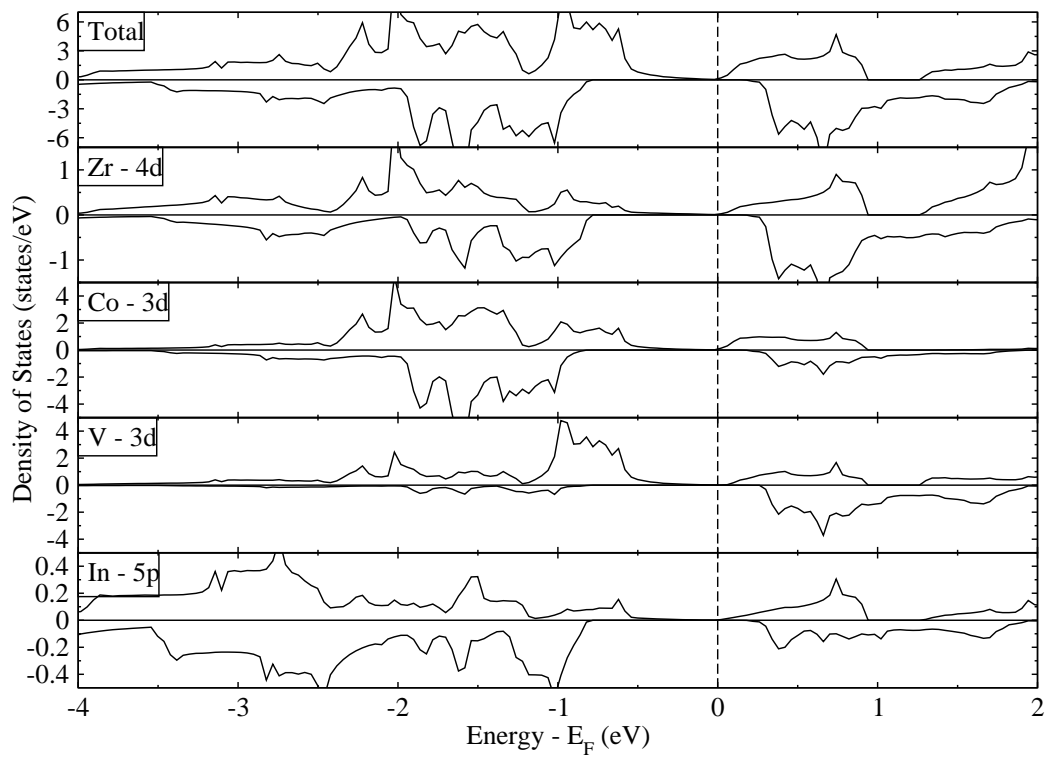


Figure 4:

2.0